

DESI and SNe: Dynamical Dark Energy, Ω_m Tension or Systematics?

Eoin Ó Colgáin¹ and M. M. Sheikh-Jabbari²

¹*Atlantic Technological University, Ash Lane, Sligo, Ireland*

²*School of Physics, Institute for Research in Fundamental Sciences (IPM), P.O.Box 19395-5531, Tehran, Iran*

Dark Energy Spectroscopic Instrument (DESI) observations, when combined with Cosmic Microwave Background (CMB) and Type Ia supernovae (SNe), have led to statistically significant dynamical dark energy (DDE) claims. In this letter we reconstruct Λ CDM parameter Ω_m from the w_0w_a CDM cosmologies advocated by the DESI collaboration. We identify i) a mild increasing Ω_m trend at high redshifts and ii) a sharp departure from Λ CDM at low redshift. The latter, which is statistically significant, is driven by SNe that are $1.9\sigma - 2.5\sigma$ discrepant with DESI full-shape galaxy clustering in overlapping redshift ranges. We identify a low redshift subsample of the Dark Energy Survey (DES) SNe sample that is discrepant with DESI at 3.4σ despite both observables probing the same effective redshift. This “ Ω_m tension” may point to unexplored systematics. SNe and BAO/full-shape modeling should not disagree on Ω_m at the same effective redshift. If they do, DDE claims are premature.

INTRODUCTION

Confronted by persistent Λ CDM tensions [1–3], notably H_0 [4–9] and S_8 tensions [4, 10–15], the simplest deduction one makes is that the Λ CDM cosmological parameters cannot be constant. More precisely, if the tensions are physical in origin - not due to systematics - the model fitting parameters must exhibit redshift-dependence. The model has broken down. Inspired by H_0 tension [4–9] and strongly lensed quasars [16, 17], in 2020 it was argued that H_0 decreases with effective redshift [18]. Subsequently, a mathematical explanation was given [19] and the observation was confirmed by independent groups, independent datasets and independent methods [20–26].

In 2022, despite no discussion of an “ Ω_m tension” at the time, leveraging a well-recognized anti-correlation between the Hubble constant H_0 and the matter density parameter Ω_m in the Λ CDM model, coupled with an existing quasar anomaly [27, 28], it was argued that Ω_m increases as we increase the effective redshift [23, 24] (see also [29]). Note, if Ω_m is not a constant, then the S_8 anomaly/tension, a discrepancy in $S_8 := \sigma_8 \sqrt{\Omega_m/0.3}$ deductions from different observations/datasets [4, 10–15], is expected. In 2023, following precursor studies [30–32],¹ it was proposed that S_8 increases with effective redshift [35]. As noted in [36], this trend was subsequently observed in cluster number counts [37], cross-correlations of DESI galaxies with CMB lensing [38] and DESI full-shape galaxy clustering [39, 40] (see also [41–43]).² See [44] for an overview of the redshift-dependent Λ CDM parameter claims.

In 2024 DESI released baryon acoustic oscillation (BAO) results [45–47], which highlighted a discrepancy in the inferred Ω_m values from BAO, CMB [4] and different combinations of Type Ia SNe, including Pantheon+ [48, 49], Union3

[50] and DES samples [51, 52]. It has been claimed in [47] that this “ Ω_m tension” across datasets can be modeled as a statistically significant dynamical dark energy (DDE) parametrized through w_0w_a CDM model [47]. Importantly, the signal persists when one replaces DESI BAO [45–47] with DESI full-shape galaxy clustering [39, 40]. Although one may eschew the Λ CDM model and focus on the w_0w_a CDM model, it is prudent to confirm that the DDE signal also manifests itself as a redshift-dependent Ω_m parameter in the Λ CDM model. To that end, we observed that a $\sim 2\sigma$ DDE signal in the DES sample alone [51, 52] can be translated into an increasing Ω_m trend with effective redshift [53], otherwise one would arrive at a contradiction.

This letter is inspired in part by a recent mapping [54] of the *mock data* based on the w_0w_a CDM cosmologies preferred by BAO+CMB+SNe [47] back into the Λ CDM model. Unfortunately, the paper overlooks the evident redshift-dependence when *observed data* is mapped back to the Λ CDM model, as outlined in the opening 2 paragraphs. This letter, in part, is intended to set the record straight. Concretely, we confirm that, irrespective of the SNe dataset, once the DDE w_0w_a CDM cosmologies are mapped back to the Ω_m parameter, one finds an increasing trend of Ω_m at higher redshifts. *This provides visual confirmation of earlier claims [23, 24] (see also [55]).*

More notably, one also finds a statistically significant departure from the constant Ω_m Λ CDM behavior at low redshift. As we argue, this departure is driven by the SNe samples. Compared to recent DESI full-shape galaxy clustering of a low redshift Bright Galaxy Survey (BGS) [40], the discrepancy with SNe in closely related redshifts we estimate at the $\sim 2\sigma$ level irrespective of the SNe dataset. Given the higher effective redshift of the DES sample, cropping the sample, we find that viewed through the Λ CDM lens, DES and DESI are *inconsistent at $\sim 3.4\sigma$ at the same effective redshift*. Our letter highlights the dangers of combining datasets in a DDE framework [39, 47] without first checking that the observables are consistent where they probe the same effective redshift. See [55] for earlier related comments.

¹ This is also predated by a late-time integrated Sachs-Wolfe effect anomaly [33, 34], which points to weaker/stronger growth at lower/higher redshifts.

² Fig. 14 of [40] confirms that SDSS and DESI agree high redshift $f\sigma_8(z)$ constraints are larger than Planck. If low redshift constraints are lower (to be seen), DESI will confirm the claim in [35], which is based on archival data, using better quality data from a single survey/telescope.

ANALYSIS

We begin our analysis by explaining the role of CMB when combined with observables, such as SNe and BAO that directly probe the late Universe. The CMB constrains the shift parameters R, l_A [56]:

$$R = \sqrt{\Omega_m H_0^2} \frac{D_M(z_*)}{c}, \quad l_A = (1 + z_*) \frac{\pi D_M(z_*)}{r_s(z_*)}, \quad (1)$$

$$D_M(z_*) := c \int_0^{z_*} \frac{dz}{H(z)}, \quad r_s(z_*) := \int_{z_*}^{\infty} \frac{c_s dz}{H(z)},$$

where $r_s(z_*)$ is the comoving sound horizon and $D_M(z_*)$ is the comoving angular diameter distance defined at the photon-decoupling surface redshift, $z_* \approx 1100$. Although both R and l_A depend on the cosmological parameters, only $D_M(z_*)$ is sensitive to the late Universe Hubble parameter $H(z)$.

As noted in [57], since $D_M(z_*)$ is an integrated quantity through to z_* , one can easily improve the fit by introducing features in $H(z)$, for example wiggles, where there are no direct observational constraints. This means that CMB cannot drive a DDE signal, but it can respond to Λ CDM deviations driven by BAO and SNe. To stress this point further, we note from Table 3 of [47] that DESI BAO combined with both CMB and a BBN prior leads to $\sim 2\sigma$ deviation from Λ CDM,³ thus confirming that CMB is not driving the signal. This is in line with mathematical expectations [57]. Having eliminated CMB as the origin of the DDE signal, we turn our focus to BAO and SNe.

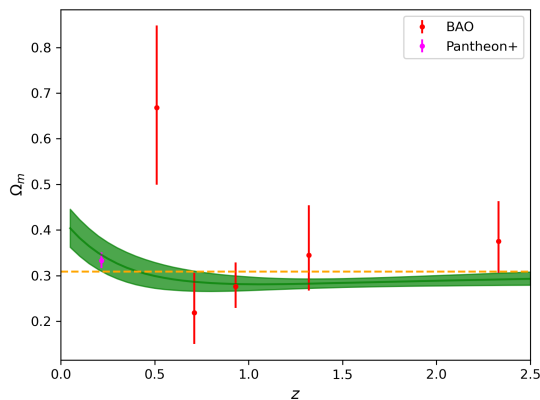


FIG. 1. Inferred values of Ω_m when the BAO+PantheonPlus+CMB $w_0 w_a$ CDM cosmology from Table I is mapped back to Λ CDM. Shaded green intervals correspond to 68% confidence intervals plotted alongside the Pantheon+ constraint and constraints inferred from DESI anisotropic BAO. The orange dashed line denotes the asymptotic value $\Omega_m = 0.3085$.

Given the best-fit $w_0 w_a$ CDM cosmologies in Table I, one can map the cosmologies back into the Λ CDM parameter Ω_m as follows.⁴ First, we break up the redshift range $z \in [0.05, 2.5]$ into discrete values z_i separated uniformly by $\Delta z = 0.05$. At each z_i we generate 10,000 new values of $(H_0, \Omega_m, w_0, w_a)$ in normal distributions about the central values from Table I using the 68% confidence intervals (errors) as standard deviations. In the case of w_a , where the errors are not symmetric, for simplicity we symmetrize the errors by adopting the largest error; this tweak can only make our analysis more conservative. From the resulting $(H_0, \Omega_m, w_0, w_a)$ array, one can construct a distribution of $D_M(z_i)$ and $D_H(z_i)$ values, where $D_H(z) := c/H(z)$. Next, following the methodology from [23, 55], we translate these distributions into an Ω_m distribution by solving the equation

$$\frac{D_M(z_i)}{D_H(z_i)} = E(z_i) \int_0^{z_i} \frac{dz}{E(z)}, \quad (2)$$

$$E(z) = \sqrt{1 - \Omega_m + \Omega_m(1+z)^3}.$$

Note that $D_M(z_i)/D_H(z_i)$ ratio is only a function of Ω_m in the Λ CDM model, and more generally, does not depend on H_0 . From the resulting Ω_m distribution we identify a median, 16th and 84th percentile at each z_i . This leads to the green curved bands in Fig. 1 - Fig. 4.

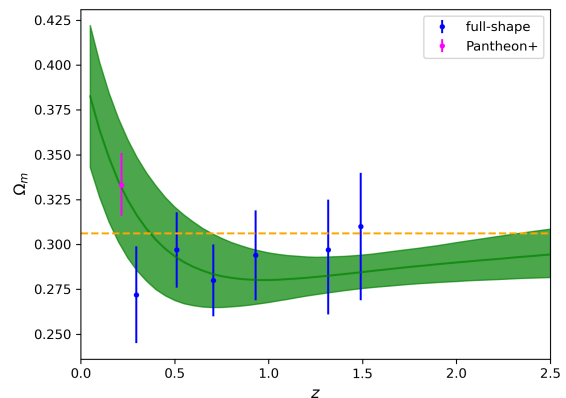


FIG. 2. Inferred values of Ω_m when the Full-Shape+PantheonPlus+CMB cosmology from Table I is mapped back to Λ CDM. Shaded green intervals correspond to 68% confidence intervals plotted alongside the Pantheon+ constraint and constraints inferred from DESI full-shape galaxy clustering. The orange dashed line denotes the asymptotic value $\Omega_m = 0.3061$.

At this point we have our first result. These observations are overlooked when one focuses on datasets without considering redshift, e. g. [54]. Let us begin with the basics. Given that we have injected a $w_0 w_a$ CDM cosmology that is distinct from

³ Concretely, from DESI+CMB one gets $w_0 = -0.45^{+0.34}_{-0.21}$, $w_a = -1.79^{+0.48}_{-1.0}$ and from DESI+BBN+ θ_* $w_0 = -0.53^{+0.42}_{-0.22}$, $w_a < -1.08$.

⁴ While there may be other ways to do this, our methodology here is mathematically exact with no approximation.

Data	H_0 [km/s/Mpc]	Ω_m	w_0	w_a
BAO+PantheonPlus+CMB	68.03 ± 0.77	0.3085 ± 0.0068	-0.827 ± 0.063	$-0.75^{+0.29}_{-0.25}$
Full-Shape+PantheonPlus+CMB	68.34 ± 0.67	0.3061 ± 0.0064	-0.858 ± 0.061	$-0.68^{+0.27}_{-0.23}$
BAO+DES+CMB	67.24 ± 0.66	0.3160 ± 0.0065	-0.727 ± 0.067	$-1.05^{+0.31}_{-0.27}$
Full-Shape+DES+CMB	67.48 ± 0.62	0.3142 ± 0.0063	-0.761 ± 0.065	$-0.96^{+0.30}_{-0.26}$

TABLE I.

Λ CDM at the $\sim 2 - 4\sigma$ level, one should not expect a constant Ω_m . In particular, the Ω_m curve shows a pronounced deviation from constant Ω_m at low redshifts with a less pronounced deviation from constant Ω_m at higher redshifts. Throughout, the orange dashed line denotes the Ω_m value from the relevant w_0w_a CDM cosmology in Table I and we have confirmed that the green curve converges from below to this value at higher redshifts, in line with expectations. The increasing Ω_m trend at higher redshifts is consistent with the claims from independent observables [23, 24]. The same trend is seen in the BAO in Fig. 1 and Fig. 3, once one ignores the obvious “statistical fluctuation” outlier in LRG data at $z = 0.51$ [55] (see also DESI [47] for related comments).⁵ The reader should note that this statistical fluctuation has disappeared in DESI full-shape galaxy clustering results, as expected.

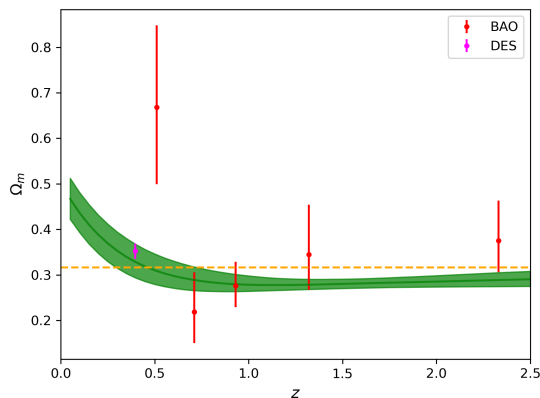


FIG. 3. Inferred values of Ω_m when the BAO+DES+CMB cosmology from Table I is mapped back to Λ CDM. Shaded green intervals correspond to 68% confidence intervals plotted alongside the DES constraint and constraints inferred from DESI anisotropic BAO. The orange dashed line denotes the asymptotic value $\Omega_m = 0.3160$.

⁵ A prediction for DESI Λ CDM results that Ω_m increases with effective redshift was made in [55]. This is clearly borne out in i) the Ω_m reconstructed from the w_0w_a CDM model and ii) DESI full-shape galaxy clustering results [40], admittedly at low significance. On the latter point, the shift between the lowest Ω_m at the lowest redshift and the highest Ω_m at the highest redshift is only $\sim 0.8\sigma$. Furthermore, it is clear that one can safely interpolate a horizontal line through the green curves for $z \gtrsim 0.4$, so any departure from Λ CDM behaviour is currently marginal. Future DESI data may resolve this feature.

We now focus on an important fact: the pronounced deviation from constant Ω_m at low redshift. It is obvious that this cannot be attributed to BAO, because we see the same feature in the full-shape modeling in Fig. 2 and Fig. 4. Moreover, even in the full-shape modeling, the green curve fails to track the lowest redshift Bright Galaxy Sample (BGS) constraint [40]. Thus, one pinpoints SNe as the culprit. In Fig. 1 and Fig. 2 we plot the Pantheon+ constraint, $\Omega_m = 0.334 \pm 0.018$ [49], at the effective redshift, $\bar{z} = 0.217$, for the full SNe sample. Here, we define our effective redshift through a weighted sum of the errors:

$$\bar{z} = \frac{\sum_{i=1}^N z_i / \sigma_i^2}{\sum_{i=1}^N 1 / \sigma_i^2}. \quad (3)$$

Given that Pantheon+ has 741 from 1701 SNe with $z < 0.1$, it is expected that Pantheon+ has a low effective redshift. While not at the same effective redshift, the discrepancy between the Pantheon+ constraint in magenta in Fig. 2 and the BGS constraint at $\bar{z} = 0.295$, $\Omega_m = 0.272 \pm 0.027$ [40], is 1.9σ . It is interesting to note that the Pantheon+ Ω_m value coincides with the median of the Ω_m values reconstructed from the corresponding w_0w_a CDM model.

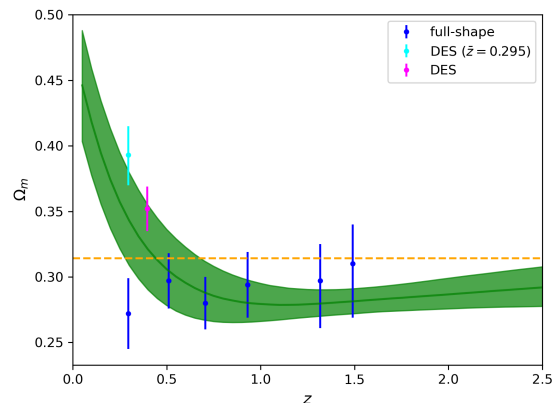


FIG. 4. Inferred values of Ω_m when the Full-Shape+DES+CMB cosmology from Table I is mapped back to Λ CDM. Shaded green intervals correspond to 68% confidence intervals plotted alongside the DES full sample constraint (magenta), DES subsample constraint (cyan) and constraints inferred from DESI full-shape galaxy clustering. The orange dashed line denotes the asymptotic value $\Omega_m = 0.3142$.

Replacing Pantheon+ SNe with DES allows us to take the

comparison with full-shape modeling further. Although the DES sample overlaps with Pantheon+ through 194 low redshift SNe, $z \lesssim 0.1$, the DES full sample has a much higher effective redshift, $\bar{z} = 0.397$. We have plotted the full sample constraint, $\Omega_m = 0.352 \pm 0.017$ [51], in magenta in Fig. 3 and Fig. 4, where it is clear that the sample explains the low redshift deviation from constant Ω_m . The effective redshift is between $\bar{z} = 0.295$ and $\bar{z} = 0.510$ probed by BGS and luminous red galaxies (LRG) tracers [40]. The discrepancy between DES SNe and these observables are $\sim 2.5\sigma$ and $\sim 2\sigma$, respectively.

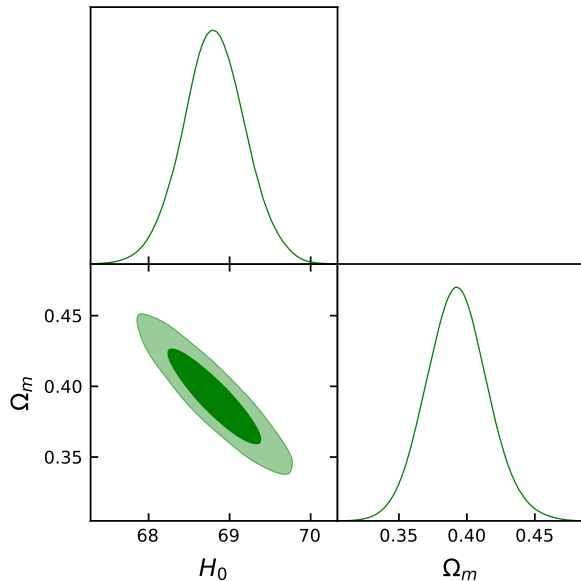


FIG. 5. Visual confirmation that DES SNe with $z < 0.597$ and an effective redshift $\bar{z} = 0.295$ lead to the constraint $\Omega_m = 0.393^{+0.022}_{-0.023}$.

However, now we can remove the higher redshift DES SNe to construct a sample with the same effective redshift as the BGS Ω_m constraint. Concretely, we restrict the DES sample to $z < 0.597$ to get the same effective redshift $\bar{z} = 0.295$. The resulting DES constraint is $\Omega_m = 0.393^{+0.022}_{-0.023}$ from Fig. 5, which is 3.4σ removed from BGS. *We stress that the DES sample and DESI full-shape constraints are in tension where the samples share the same effective redshift.* This highlights the obvious shortcoming of glibly combining samples into a DDE framework, such as the w_0w_a CDM model [39, 47].⁶

As a final comment, it is clear that full-shape modeling of galaxy clusters has led to Ω_m constraints that are more consistent with Λ CDM, modulo the residual increasing Ω_m trend with redshift. In principle, the conspicuous BAO outlier at

$z = 0.51$ in Fig. 1 and Fig. 3 can drive the DDE signal for BAO+CMB from Table 3 of [47] (see [53]). The analogous data combination for full-shape+CMB does not appear in Table 2 of [39], but if the results could be found, then this may add further support to our claim here that SNe drive the greatest deviation from constant Ω_m Λ CDM behavior. It would be most transparent to remove the SNe from Fig. 2 and Fig. 4 to see if the low redshift deviation persists.

DISCUSSION

The DESI+CMB+SNe DDE signals raise perplexing theoretical questions. First and foremost, any dark energy model that crosses the phantom divide $w = -1$ is theoretically more of a challenge [58], which would consign quintessence [59–61], the simplest field theory of dark energy, to the bin. Secondly, we note that a high local H_0 [5–9] is also challenging to any dark energy field theory with an equation of state $w(z=0) = w_0 > -1$ [62, 63]. This statement places the DESI DDE claim at odds with H_0 tension. Even within the Horndeski class, this would push one to more exotic models in the class [64, 65].

As advocated recently in [54], it is instructive to map the DDE w_0w_a CDM cosmologies preferred by DESI+CMB+SNe back into the Λ CDM model. While [54] is a step in the right direction, it misses the point that the focus should be on effective redshift, rather than on different datasets. We know this because, *within the existing literature, mapping observed data back into the parameters of the Λ CDM model has led to trends whereby H_0 decreases with effective redshift [18, 19, 21–26], Ω_m increases with effective redshift [23, 24, 53, 55]* (a trend evident in DESI full-shape modeling constraints at low significance) and σ_8/S_8 increases with effective redshift [30–32, 35–38, 41–43]. As initially argued for H_0 [19], these trends are expected signatures of Λ CDM model breakdown.

We uncovered two interesting redshift-dependent features in our Λ CDM Ω_m reconstructions of the w_0w_a CDM model preferred by DESI+CMB+SNe data. The first is that there is an increasing trend of Ω_m with redshift at higher redshifts. This is in line with trends reported in the literature [23, 24, 29, 53, 55]. The second and more noticeable feature is the departure from Λ CDM behavior at low redshifts $z \lesssim 0.5$. As we have argued, this is primarily driven by SNe samples that possess low effective redshifts and not by CMB or DESI data. Recent observations from DESI full-shape modeling of galaxy cluster are shifted lower than SNe by $\sim 2\sigma$ at similar effective redshift. At $\sim 2\sigma$, this may not be such a glaring problem, but as we have shown, one can tailor the DES SNe sample by removing higher redshift SNe to construct a sample with the same effective redshift as the BGS constraint. The constraints are inconsistent at $> 3\sigma$ at the same redshift, indicating that DES SNe and DESI full-shape modeling cannot be tracing the same Λ CDM Universe. The key take-home is that this inconsistency is far from obvious when one combines DESI observations with CMB and SNe in the context of the

⁶ One can translate this Ω_m tension back to distances using the Λ CDM cosmology, thereby confirming that DESI and DES disagree on the distance at $\bar{z} = 0.295$. We do not expect the constraint on this distance to be greatly affected when one changes the cosmology as SNe apparent magnitudes track distances and not cosmological parameters.

w_0w_a CDM model.

The big picture here is that it has been argued that H_0 and S_8 tensions point to a crisis in cosmology. As argued initially in [19], differences in cosmological parameters at different effective redshifts can be reconciled if the Λ CDM model has broken down. Nevertheless, differences in cosmological parameters between observables at the same effective redshift are more serious; they raise the possibility that the observables are not tracking the same physical Universe.

ACKNOWLEDGEMENTS

We thank Özgür Akarsu, Purba Mukherjee and Anjan Sen for related discussions. This article/publication is based upon work from COST Action CA21136 – “Addressing observational tensions in cosmology with systematics and fundamental physics (CosmoVerse)”, supported by COST (European Cooperation in Science and Technology). The work of MMSHJ is in part supported by the INSF grant No 4026712.

-
- [1] E. Di Valentino, O. Mena, S. Pan, L. Visinelli, W. Yang, A. Melchiorri, D. F. Mota, A. G. Riess, and J. Silk, *Class. Quant. Grav.* **38**, 153001 (2021), arXiv:2103.01183 [astro-ph.CO].
- [2] L. Perivolaropoulos and F. Skara, *New Astron. Rev.* **95**, 101659 (2022), arXiv:2105.05208 [astro-ph.CO].
- [3] E. Abdalla *et al.*, *JHEAp* **34**, 49 (2022), arXiv:2203.06142 [astro-ph.CO].
- [4] N. Aghanim *et al.* (Planck), *Astron. Astrophys.* **641**, A6 (2020), [Erratum: *Astron. Astrophys.* 652, C4 (2021)], arXiv:1807.06209 [astro-ph.CO].
- [5] A. G. Riess *et al.*, *Astrophys. J. Lett.* **934**, L7 (2022), arXiv:2112.04510 [astro-ph.CO].
- [6] W. L. Freedman, *Astrophys. J.* **919**, 16 (2021), arXiv:2106.15656 [astro-ph.CO].
- [7] D. W. Pesce *et al.*, *Astrophys. J. Lett.* **891**, L1 (2020), arXiv:2001.09213 [astro-ph.CO].
- [8] J. P. Blakeslee, J. B. Jensen, C.-P. Ma, P. A. Milne, and J. E. Greene, *Astrophys. J.* **911**, 65 (2021), arXiv:2101.02221 [astro-ph.CO].
- [9] E. Kourkchi, R. B. Tully, G. S. Anand, H. M. Courtois, A. Dupuy, J. D. Neill, L. Rizzi, and M. Seibert, *Astrophys. J.* **896**, 3 (2020), arXiv:2004.14499 [astro-ph.GA].
- [10] C. Heymans *et al.*, *Mon. Not. Roy. Astron. Soc.* **432**, 2433 (2013), arXiv:1303.1808 [astro-ph.CO].
- [11] S. Joudaki *et al.*, *Mon. Not. Roy. Astron. Soc.* **465**, 2033 (2017), arXiv:1601.05786 [astro-ph.CO].
- [12] M. A. Troxel *et al.* (DES), *Phys. Rev. D* **98**, 043528 (2018), arXiv:1708.01538 [astro-ph.CO].
- [13] C. Hikage *et al.* (HSC), *Publ. Astron. Soc. Jap.* **71**, 43 (2019), arXiv:1809.09148 [astro-ph.CO].
- [14] M. Asgari *et al.* (KiDS), *Astron. Astrophys.* **645**, A104 (2021), arXiv:2007.15633 [astro-ph.CO].
- [15] T. M. C. Abbott *et al.* (DES), *Phys. Rev. D* **105**, 023520 (2022), arXiv:2105.13549 [astro-ph.CO].
- [16] K. C. Wong *et al.*, *Mon. Not. Roy. Astron. Soc.* **498**, 1420 (2020), arXiv:1907.04869 [astro-ph.CO].
- [17] M. Millon *et al.*, *Astron. Astrophys.* **639**, A101 (2020), arXiv:1912.08027 [astro-ph.CO].
- [18] C. Krishnan, E. Ó Colgáin, Ruchika, A. A. Sen, M. M. Sheikh-Jabbari, and T. Yang, *Phys. Rev. D* **102**, 103525 (2020), arXiv:2002.06044 [astro-ph.CO].
- [19] C. Krishnan, E. Ó Colgáin, M. M. Sheikh-Jabbari, and T. Yang, *Phys. Rev. D* **103**, 103509 (2021), arXiv:2011.02858 [astro-ph.CO].
- [20] M. G. Dainotti, B. De Simone, T. Schiavone, G. Montani, E. Rinaldi, and G. Lambiase, *Astrophys. J.* **912**, 150 (2021), arXiv:2103.02117 [astro-ph.CO].
- [21] M. G. Dainotti, B. De Simone, T. Schiavone, G. Montani, E. Rinaldi, G. Lambiase, M. Bogdan, and S. Ugale, *Galaxies* **10**, 24 (2022), arXiv:2201.09848 [astro-ph.CO].
- [22] J.-P. Hu and F. Y. Wang, *Mon. Not. Roy. Astron. Soc.* **517**, 576 (2022), arXiv:2203.13037 [astro-ph.CO].
- [23] E. Ó Colgáin, M. M. Sheikh-Jabbari, R. Solomon, G. Bargiacchi, S. Capozziello, M. G. Dainotti, and D. Stojkovic, *Phys. Rev. D* **106**, L041301 (2022), arXiv:2203.10558 [astro-ph.CO].
- [24] E. Ó Colgáin, M. M. Sheikh-Jabbari, R. Solomon, M. G. Dainotti, and D. Stojkovic, *Phys. Dark Univ.* **44**, 101464 (2024), arXiv:2206.11447 [astro-ph.CO].
- [25] X. D. Jia, J. P. Hu, and F. Y. Wang, *Astron. Astrophys.* **674**, A45 (2023), arXiv:2212.00238 [astro-ph.CO].
- [26] X. D. Jia, J. P. Hu, and F. Y. Wang, (2024), arXiv:2406.02019 [astro-ph.CO].
- [27] G. Risaliti and E. Lusso, *Nature Astron.* **3**, 272 (2019), arXiv:1811.02590 [astro-ph.CO].
- [28] E. Lusso *et al.*, *Astron. Astrophys.* **642**, A150 (2020), arXiv:2008.08586 [astro-ph.GA].
- [29] E. Ó Colgáin, M. M. Sheikh-Jabbari, and L. Yin, (2024), arXiv:2405.19953 [astro-ph.CO].
- [30] M. White *et al.*, *JCAP* **02**, 007 (2022), arXiv:2111.09898 [astro-ph.CO].
- [31] C. García-García, J. R. Zapatero, D. Alonso, E. Bellini, P. G. Ferreira, E.-M. Mueller, A. Nicola, and P. Ruiz-Lapuente, *JCAP* **10**, 030 (2021), arXiv:2105.12108 [astro-ph.CO].
- [32] M. Esposito, V. Iršič, M. Costanzi, S. Borgani, A. Saro, and M. Viel, *Mon. Not. Roy. Astron. Soc.* **515**, 857 (2022), arXiv:2202.00974 [astro-ph.CO].
- [33] A. Kovács *et al.* (DES), *Mon. Not. Roy. Astron. Soc.* **484**, 5267 (2019), arXiv:1811.07812 [astro-ph.CO].
- [34] A. Kovács, R. Beck, A. Smith, G. Rácz, I. Csabai, and I. Szapudi, *Mon. Not. Roy. Astron. Soc.* **513**, 15 (2022), arXiv:2107.13038 [astro-ph.CO].
- [35] S. A. Adil, O. Akarsu, M. Malekjani, E. Ó Colgáin, S. Pourrajahi, A. A. Sen, and M. M. Sheikh-Jabbari, *Mon. Not. Roy. Astron. Soc.* **528**, L20 (2023), arXiv:2303.06928 [astro-ph.CO].
- [36] O. Akarsu, E. Ó Colgáin, A. A. Sen, and M. M. Sheikh-Jabbari, (2024), arXiv:2410.23134 [astro-ph.CO].
- [37] E. Artis, E. Bulbul, *et al.* (SRG/eROSITA), arXiv e-prints, arXiv:2410.09499 (2024), arXiv:2410.09499 [astro-ph.CO].
- [38] F. J. Qu *et al.* (ACT), arXiv e-prints, arXiv:2410.10808 (2024), arXiv:2410.10808 [astro-ph.CO].
- [39] A. G. Adame *et al.* (DESI), (2024), arXiv:2411.12022 [astro-ph.CO].
- [40] A. G. Adame *et al.* (DESI), (2024), arXiv:2411.12021 [astro-ph.CO].
- [41] I. Tutusaus, C. Bonvin, and N. Grimm, arXiv e-prints, arXiv:2312.06434 (2023), arXiv:2312.06434 [astro-ph.CO].
- [42] S. Manna and S. Desai, *Eur. Phys. J. C* **84**, 661 (2024), arXiv:2406.10931 [astro-ph.CO].

- [43] N. Sailer *et al.* (ACT), arXiv e-prints , arXiv:2407.04607 (2024), arXiv:2407.04607 [astro-ph.CO].
- [44] O. Akarsu, E. Ó Colgáin, A. A. Sen, and M. M. Sheikh-Jabbari, *Universe* **10**, 305 (2024), arXiv:2402.04767 [astro-ph.CO].
- [45] A. G. Adame *et al.* (DESI), (2024), arXiv:2404.03000 [astro-ph.CO].
- [46] A. G. Adame *et al.* (DESI), (2024), arXiv:2404.03001 [astro-ph.CO].
- [47] A. G. Adame *et al.* (DESI), arXiv e-prints , arXiv:2404.03002 (2024), arXiv:2404.03002 [astro-ph.CO].
- [48] D. Scolnic *et al.*, *Astrophys. J.* **938**, 113 (2022), arXiv:2112.03863 [astro-ph.CO].
- [49] D. Brout *et al.*, *Astrophys. J.* **938**, 110 (2022), arXiv:2202.04077 [astro-ph.CO].
- [50] D. Rubin *et al.*, (2023), arXiv:2311.12098 [astro-ph.CO].
- [51] T. M. C. Abbott *et al.* (DES), *Astrophys. J. Lett.* **973**, L14 (2024), arXiv:2401.02929 [astro-ph.CO].
- [52] B. O. Sánchez *et al.* (DES), (2024), arXiv:2406.05046 [astro-ph.CO].
- [53] E. Ó Colgáin, S. Pourojaghi, and M. M. Sheikh-Jabbari, arXiv e-prints , arXiv:2406.06389 (2024), arXiv:2406.06389 [astro-ph.CO].
- [54] X. T. Tang, D. Brout, T. Karwal, C. Chang, V. Miranda, and M. Vincenzi, (2024), arXiv:2412.04430 [astro-ph.CO].
- [55] E. Ó Colgáin, M. G. Dainotti, S. Capozziello, S. Pourojaghi, M. M. Sheikh-Jabbari, and D. Stojkovic, (2024), arXiv:2404.08633 [astro-ph.CO].
- [56] E. Komatsu *et al.* (WMAP), *Astrophys. J. Suppl.* **180**, 330 (2009), arXiv:0803.0547 [astro-ph].
- [57] O. Akarsu, E. Ó Colgáin, E. Özulker, S. Thakur, and L. Yin, *Phys. Rev. D* **107**, 123526 (2023), arXiv:2207.10609 [astro-ph.CO].
- [58] A. Vikman, *Phys. Rev. D* **71**, 023515 (2005), arXiv:astro-ph/0407107.
- [59] B. Ratra and P. J. E. Peebles, *Phys. Rev. D* **37**, 3406 (1988).
- [60] C. Wetterich, *Nucl. Phys. B* **302**, 668 (1988), arXiv:1711.03844 [hep-th].
- [61] E. J. Copeland, M. Sami, and S. Tsujikawa, *Int. J. Mod. Phys. D* **15**, 1753 (2006), arXiv:hep-th/0603057.
- [62] A. Banerjee, H. Cai, L. Heisenberg, E. Ó Colgáin, M. M. Sheikh-Jabbari, and T. Yang, *Phys. Rev. D* **103**, L081305 (2021), arXiv:2006.00244 [astro-ph.CO].
- [63] B.-H. Lee, W. Lee, E. Ó Colgáin, M. M. Sheikh-Jabbari, and S. Thakur, *JCAP* **04**, 004 (2022), arXiv:2202.03906 [astro-ph.CO].
- [64] A. De Felice and S. Tsujikawa, *JCAP* **02**, 007 (2012), arXiv:1110.3878 [gr-qc].
- [65] J. Matsumoto, *Phys. Rev. D* **97**, 123538 (2018), arXiv:1712.10015 [gr-qc].